

# A matrix approach to grazing-incidence X-ray diffraction in multilayers

S.A. Stepanov<sup>1,\*</sup>, U. Pietsch<sup>2</sup>, G.T. Baumbach<sup>3</sup>

<sup>1</sup> Institute for Nuclear Problems, Bobruiskaya 11, SU-220050 Minsk, Belarus

<sup>2</sup> Universität Potsdam, Am Neuen Palais 10, D-14415 Potsdam, Germany (Fax: +49(331) 9771286)

<sup>3</sup> Institute Laue-Langevin, 156X, F-38042 Grenoble Cedex, France

Received: 20 June 1994 / Revised version: 8 August 1994

**Abstract.** A method for computation of X-ray grazing-incidence diffraction (GID) in multilayers and superlattices is presented. The method is based on X-ray dynamical diffraction theory and a matrix from a boundary equations and provides a simple numerical solution of the problem. The application of the method to simulating GID measurements taken from AlAs/GaAs superlattice (20 periods of 14.6 nm AlAs and 6.8 nm GaAs) demonstrates the principal validity of the theory. A perfect matching between the theory and the experiment requires the real-structure effects of sample to be taken into account.

**PACS:** 61.10; 68.65

## 1. Introduction

In recent years, the X-ray grazing-incidence diffraction method (GID) has been effectively applied to the studies of semiconductor multilayers [1]–[9]. However, until now, it has been possible to give a theoretical interpretation only to certain particular cases of these measurements. For example, a theoretical analysis of GID in a structure composed by a series of amorphous layers grown on crystal surface was carried out [1]. A theory of the case of extremely asymmetric GID was developed [2]. The GID in strongly periodic superlattices was analyzed [5]. A kinematical approach to GID in multilayers was proposed [4, 10]; however, it was not applicable to a high-quality multilayers because of known assumptions contained in the kinematical theory. An extension of Takagi-Taupin equations was derived in [11], but the numerical solution of these equations contained matrix exponentials and therefore the computations were very much time consuming. Besides, the solution of these differential equations might turn out to be unstable for the sharp interfaces in

multilayers. Finally, a set of linear algebraic equations of dynamical diffraction in an arbitrary sequence of multilayers was derived and suggested to be solved numerically by Gaussian method [3]. Unfortunately, this approach could not work for  $N_{\text{layers}} \geq 5$  due to rounding errors in the simultaneous numerical solution of the  $(4 \times N_{\text{layers}})$ -set of equations. Therefore, a quantitative analysis of experimental GID data taken from multilayers has not been possible until now.

Recently, a new way to solve the dynamical diffraction equations derived in [3] was independently found in [12] and [13]. It was shown that the set of  $(4 \times N_{\text{layers}})$  can be decomposed onto  $(4 \times 4)$  matrix blocks and then the numerical solution of the problem can be reduced to relatively simple operations with  $(4 \times 4)$  matrices.

In [12] the  $(4 \times 4)$  matrix approach was successfully applied to analyzing GID in ion-implanted silicon crystal. The depth profile of the implanted surface layer was subdivided into few sublayers and the scattering amplitudes in these sublayers were fitted to match the experimental data. Due to the small thickness of the analyzed layer, the validity of applying matrix method to thick layers was not analyzed.

In [13] the  $(4 \times 4)$  matrix method was developed in order to analyze GID from synthetic multilayers and superlattices. Therefore, some more general case of arbitrary sequence of amorphous and crystalline layers with different density was considered. Besides, it was shown that the  $(4 \times 4)$  matrix algorithm might diverge, when it is applied to computing GID from many layers. However, the divergence problem was overcome with the help of dynamical thick crystal approximation. With this approximation, the  $(4 \times 4)$  matrix approach was shown to be applicable to  $10^2 - 10^3$  or even more layers.

In present paper we give a new more accurate derivation of  $(4 \times 4)$  matrix method [13] and apply it for the first time to analysis of experimental GID data taken from synthetic superlattices. In Sect. 2, the  $(4 \times 4)$  matrix algorithm is derived. In Sect. 3, the dynamical thick crystal approximation is discussed. In Sect. 4, some details of GID measurements taken at HASYLAB from

\* Temporary address: MPG-AG "Röntgenbeugung", Hausvogtei-platz 5–7, D-10117 Berlin, Germany (Fax: +49(30)2004536)

AlAs/GaAs superlattices are given. In Sect. 5, the matrix algorithm is applied to computer simulation of these measurements and the obtained results are discussed.

## 2. Matrix method

Let us consider X-ray GID in a multilayered structure composed of an arbitrary sequence of amorphous and matched crystalline layers<sup>1</sup>. Within the dynamical diffraction formalism the X-ray wave fields in vacuum beyond the structure and in every layer may be written for every X-ray polarization in the following form (see [3] for more details):

$$E_o(\mathbf{r}) = \{E_0 \exp(ix\Phi_0 z) + E_s \exp(-ix\Phi_0 z)\} \exp(i\mathbf{x}_\perp \mathbf{r}_\perp) + \{E_h \exp(-ix\Phi_h z)\} \exp(i(\mathbf{x} + \mathbf{h})_\perp \mathbf{r}_\perp) \quad (1)$$

- in vacuum,

$$D_c^k(\mathbf{r}) = \left\{ \sum_{j=1}^4 D_j^k \exp(ixu_j^k z) \right\} \exp(i\mathbf{x}_\perp \mathbf{r}_\perp) + \left\{ \sum_{j=1}^4 V_j^k D_j^k \exp(ix(u_j^k + \psi)z) \right\} \times \exp(i(\mathbf{x} + \mathbf{h})_\perp \mathbf{r}_\perp) \quad (2)$$

- in crystalline layers,

$$D_a^k(\mathbf{r}) = \{D_0^k \exp(ixu_0^k z) + D_{0s}^k \exp(ixu_{0s}^k z)\} \exp(i\mathbf{x}_\perp \mathbf{r}_\perp) + \{D_h^k \exp(ix(u_h^k + \psi)z) + D_{hs}^k \exp(ix(u_{hs}^k + \psi)z)\} \exp(i(\mathbf{x} + \mathbf{h})_\perp \mathbf{r}_\perp) \quad (3)$$

- in amorphous layers.

Here  $E_0$  is the amplitude of incident wave, equal to one.  $E_s$  and  $E_h$  are that of the reflected and diffracted waves, respectively (see schematic layout in Fig. 1). Index  $k = 1, \dots, N$  denotes the index of a layer in the sequence of surface layers;  $\mathbf{x}$  is the wave vector of the incident X-ray ( $x = |\mathbf{x}|$ );  $\mathbf{h}$  is the reciprocal lattice vector in Bragg position to  $\mathbf{x}$ ;  $\Phi_0$  is the incidence angle and  $\Phi_h$  is the exit angle of the diffracted X-ray wave with respect to the crystal surface. Parameters  $u_j^k$  are the solutions of the 4th order dispersion equation of dynamical diffraction in a  $k$ -th crystalline layer ( $j = 1, \dots, 4$ ):

$$(u_j^k - \Phi_0^2 - \chi_0^k)((u_j^k + \psi)^2 - \Phi_h^2 - \chi_0^k) = \chi_h^k \chi_h^k \quad (4)$$

Parameters  $\chi_0^k, \chi_h^k, \chi_h^k$  are the Fourier components of X-ray dielectric susceptibility for a  $k$ -th layer;  $\psi = 2\delta \sin(\theta_B)$ ,  $\delta$  is the angular misorientation of  $\mathbf{h}$

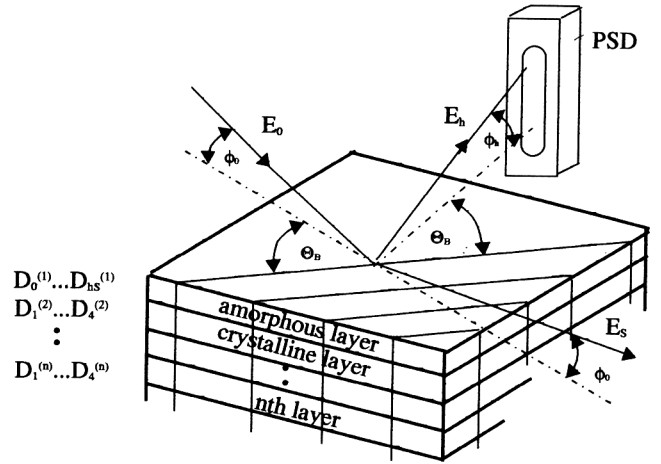


**Fig. 1.** Schematic view of X-ray grazing-incidence diffraction in multilayers.  $E_0, E_h$  are amplitudes of the incident, Bragg reflected and specularly reflected beams.  $D_1^{(n)} \dots D_4^{(n)}$  are the wavefield amplitudes in the  $n$ -th layer.  $\Phi_0$  and  $\Phi_h$  are the angles of incidence and exit,  $\theta_B$  is the Bragg angle. PSD denotes the position sensitive detector used in the experiment

with respect to the surface;  $V_j^k = (u_j^{k2} - \Phi_0^2 - \chi_0^k)/\chi_h^k$  are the ratio of the diffracted-to-transmitted amplitudes for the  $j$ -th solution of (4);  $u_{0,0s}^k = \pm \sqrt{\Phi_0^2 + \chi_0^k}$ ,  $u_{h,hs}^k = \pm \sqrt{\Phi_h^2 + \chi_0^k - \psi}$ . Four wavefields are excited in each layer. As shown in [14], Eq. (4) always has two solutions describing the amplitudes which are damped inside the structure and two which are raised (conforming to  $\text{Im} u_j > 0$  and  $\text{Im} u_j < 0$ , respectively). The latter pair is usually treated as the reflection from the lower boundary of the layer. Therefore, this pair of waves should be discarded for the last layer (the substrate).

Thus, in the case of a  $N$ -layered structure we have  $4N$  unknown wave amplitudes: 2 amplitudes in vacuum ( $E_s, E_h$ ) and  $4(N-1) + 2$  in multilayers. In order to find these amplitudes a set of  $4N$  boundary conditions has to be applied for X-ray wavefields and their derivatives at  $N$  interfaces [3]. In particular, at the vacuum-crystalline layer interface the conditions are:

$$\begin{aligned} E_0 + E_s &= \sum_{j=1}^4 D_j^1 \\ E_h &= \sum_{j=1}^4 V_j^1 D_j^1 \\ \Phi_0(E_0 - E_s) &= \sum_{j=1}^4 u_j^1 D_j^1 \\ -\Phi_h E_h &= \sum_{j=1}^4 w_j^1 D_j^1. \end{aligned} \quad (5)$$

At crystalline-crystalline, crystalline-amorphous and amorphous-amorphous interfaces the conditions have the form:

<sup>1</sup> Please note, that the mismatched layers with  $|\Delta d/d| > 10^{-4}$  can be treated as amorphous because they do not satisfy the Bragg diffraction condition simultaneously with the other layers

$$\begin{aligned}
\sum_{j=1}^4 f_j^{k(L)} D_j^k &= \sum_{j=1}^4 f_j^{k+1(U)} D_j^{k+1} \\
\sum_{j=1}^4 V_j^k f_j^{k(L)} D_j^k &= \sum_{j=1}^4 V_j^{k+1} f_j^{k+1(U)} D_j^{k+1} \\
\sum_{j=1}^4 u_j^k f_j^{k(L)} D_j^k &= \sum_{j=1}^4 u_j^{k+1} f_j^{k+1(U)} D_j^{k+1} \\
\sum_{j=1}^4 w_j^k f_j^{k(L)} D_j^k &= \sum_{j=1}^4 w_j^{k+1} f_j^{k+1(U)} D_j^{k+1}
\end{aligned} \tag{6}$$

$$\begin{aligned}
\sum_{j=1}^4 f_j^{k(L)} D_j^k &= \sum_{j=0,0s} f_j^{k+1(U)} D_j^{k+1} \\
\sum_{j=1}^4 V_j^k f_j^{k(L)} D_j^k &= \sum_{j=h,hs} f_j^{k+1(U)} D_j^{k+1} \\
\sum_{j=1}^4 u_j^k f_j^{k(L)} D_j^k &= \sum_{j=0,0s} u_j^{k+1} f_j^{k+1(U)} D_j^{k+1} \\
\sum_{j=1}^4 w_j^k f_j^{k(L)} D_j^k &= \sum_{j=h,hs} (u_j^{k+1} + \psi) f_j^{k+1(U)} D_j^{k+1}
\end{aligned} \tag{7}$$

$$\begin{aligned}
\sum_{j=0,0s} f_j^{k(L)} D_j^k &= \sum_{j=0,0s} f_j^{k+1(U)} D_j^{k+1} \\
\sum_{j=h,hs} f_j^{k(L)} D_j^k &= \sum_{j=h,hs} f_j^{k+1(U)} D_j^{k+1} \\
\sum_{j=0,0s} u_j^k f_j^{k(L)} D_j^k &= \sum_{j=0,0s} u_j^{k+1} f_j^{k+1(U)} D_j^{k+1} \\
\sum_{j=h,hs} (u_j^k + \psi) f_j^{k(L)} D_j^k &= \sum_{j=h,hs} (u_j^{k+1} + \psi) f_j^{k+1(U)} D_j^{k+1}
\end{aligned} \tag{8}$$

– and so on. Here the following notations are used:

$$w_j^k = V_j^k (u_j^k + \psi), \quad f_j^k = \exp(iu_j^k xz).$$

Indices ( $L$ ) and ( $U$ ) indicate that exponent is evaluated at the lower (upper) boundary of layer.

Rhan and Pietsch attempted to solve this set of  $4N$  equations by Gaussian method [3]. However, a more appropriate way is to rewrite the boundary equations at each interface in a matrix form [12, 13]. For this aim, we introduce 4-component vectors  $D^k$ , layers scattering matrices  $S^k$  and matrices  $A^k$  and  $B^k$  for the right and left sides of the boundary conditions:

$$D_{cr}^k = \begin{pmatrix} D_1^k \\ D_2^k \\ D_3^k \\ D_4^k \end{pmatrix}, \quad D_{am}^k = \begin{pmatrix} D_0^k \\ D_h^k \\ D_{0s}^k \\ D_{hs}^k \end{pmatrix} \tag{9}$$

$$S_{cr}^k = \begin{pmatrix} 1 & 1 & 1 & 1 \\ V_1^k & V_2^k & V_3^k & V_4^k \\ u_1^k & u_2^k & u_3^k & u_4^k \\ w_1^k & w_2^k & w_3^k & w_4^k \end{pmatrix} \tag{10}$$

$$S_{am}^k = \begin{pmatrix} 1 & 0 & 1 & 0 \\ 0 & 1 & 0 & 1 \\ u_0^k & 0 & u_{0s}^k & 0 \\ 0 & u_h^k + \psi & 0 & u_{hs}^k + \psi \end{pmatrix}$$

$$A^k = S^k F^{k(U)} \quad B^k = S^k F^{k(L)} \tag{11}$$

where  $F_{ij}^k = f_i^k \delta_{ij}$ . For the substrate layer, only the first 2 components of  $D^k$  and the first 2 rows of  $S^k$  remain and the size of  $F^k$  is  $(2 \times 2)$ .

For the fields beyond the surface a 4-component “vacuum” vector  $E^v = (E_0, E_{0h}, E_s, E_h)$  is introduced, where  $E_0 = 1$  and  $E_{0h} = 0$  are the amplitudes of incident wave incoming from 0-th and  $h$ -th wave directions. Vacuum scattering matrices  $S^v$ ,  $F^{v(L)}$  and  $B^v$  are assumed in analogous form to that for amorphous layers taking into account the condition  $\chi_0^v = \chi_h^v = 0$ .

With the help of our designations, the boundary conditions are rewritten as follows:

$$\begin{aligned}
B^v E^v &= A^1 D^1 \\
B^1 D^1 &= A^2 D^2 \\
&\dots\dots\dots \\
B^k D^k &= A^{k+1} D^{k+1} \\
&\dots\dots\dots \\
B^{N-1} D^{N-1} &= A^N D^N
\end{aligned} \tag{12}$$

where  $D^N \equiv D^s$  and  $A^N \equiv A^s$  are 2-component vector and  $(2 \times 4)$  matrix of the substrate.

So, we see that the overall set of equations is quasi-diagonal:

$$\begin{pmatrix} B^v - A^1 & 0 & 0 & \dots & 0 & 0 & 0 \\ 0 & B^1 - A^2 & 0 & \dots & 0 & 0 & 0 \\ 0 & 0 & B^2 - A^3 & \dots & 0 & 0 & 0 \\ 0 & 0 & 0 & B^3 & \dots & 0 & 0 \\ \dots & \dots & \dots & \dots & \dots & \dots & \dots \\ 0 & 0 & 0 & 0 & \dots & -A^{N-2} & 0 \\ 0 & 0 & 0 & 0 & \dots & B^{N-2} & -A^{N-1} \\ 0 & 0 & 0 & 0 & \dots & 0 & B^{N-1} - A^N \end{pmatrix} \times \begin{pmatrix} E^v \\ D^1 \\ D^2 \\ D^3 \\ \dots \\ D^{N-2} \\ D^{N-1} \\ D^N \end{pmatrix} = \begin{pmatrix} 0 \\ 0 \\ 0 \\ 0 \\ \dots \\ 0 \\ 0 \\ 0 \end{pmatrix}. \tag{13}$$

Therefore, the solution of (12) can be greatly simplified. If we begin to solve (12) starting at the last line, we arrive at:

$$E^v = (B^v)^{-1} A^1 (B^1)^{-1} \dots A^{N-1} (B^{N-1})^{-1} A^N D^s \tag{14}$$

or

$$E^v = (B^v)^{-1} (T^1 \dots T^{N-1}) A^N D^s.$$

We shall refer the products  $T^k = A^k (B^k)^{-1}$  as the transfer or  $T$ -matrices of the layers. From (11) it follows that:

$$T^k = S^k F^{k(U)} (F^{k(L)})^{-1} (S^k)^{-1} = S^k F_t^k (S^k)^{-1}. \quad (15)$$

Here  $(F_t^k)_{ij} = \exp(-iu_j^k x t^k) \delta_{ij}$ ,  $t^k = z^{k(L)} - z^{k(U)}$  is the thickness of  $k$ -th layer. If the thickness of layer tends to zero, then:

$$F_t^k \rightarrow I, \quad T^k \rightarrow S^k (S^k)^{-1} = I$$

– i.e.  $T$ -matrix of an infinitely thin layer tends to a diagonal unit matrix.

Equation (14) has a clear physical sense. If all  $t^k = 0$ , Eq. (14) coincides with the case of the GID of a perfect crystal. If there are layers on the crystal surface, the substrate matrix is modified by a product of  $T$ -matrices of all of these layers:

$$\tilde{S}^s = T^1 \dots T^{N-1} S^s F^{s(U)}. \quad (16)$$

Note that Eq. (16) is automatically reduced to that for the perfect crystal if all the layers have the same structure. In this case:

$$\tilde{S}^s = S^s \underbrace{(F_t^1 \dots F_t^{N-1})}_{(F^{s(U)})^{-1}} \underbrace{(S^s)^{-1} S^s}_{I} F^{s(U)} = S^s. \quad (17)$$

In general case Eq. (14) with account of (16) provides a set of 4 equations with respect to 4 unknown amplitudes:  $E_0$ ,  $E_s$ ,  $D_1^s$ , and  $D_2^s$ :

$$E^v = (B^v)^{-1} \tilde{S}^s D^s \equiv X D^s \quad (18)$$

or:

$$\begin{cases} X_{11} D_1^s + X_{12} D_2^s = 1 \\ X_{21} D_1^s + X_{22} D_2^s = 0 \\ X_{31} D_1^s + X_{32} D_2^s = E_s \\ X_{41} D_1^s + X_{42} D_2^s = E_h \end{cases} \quad (18a)$$

The solution of (18) is straightforward:

$$E_s = \frac{X_{31} X_{22} - X_{32} X_{21}}{X_{11} X_{22} - X_{12} X_{21}}, \quad (19)$$

$$E_h = \frac{X_{41} X_{22} - X_{42} X_{21}}{X_{11} X_{22} - X_{12} X_{21}}.$$

We see the advantage of the proposed approach is the absence of any operations with matrices greater than  $(4 \times 4)$ . Therefore, the total solution is expected to be reliable in numerical implementation.

To realize the algorithm numerically, one has to:

- compute  $S^k$ ,
- find their inverses by any conventional method of numeric algebra,

- compute  $T^k$  and their product,
- evaluate  $X_{ij}$  and  $E_s$ ,  $E_h$  according to (18) and (19).

The reflection coefficients are found according to the formulae:<sup>2</sup>

$$P_s = |E_s|^2 \quad (20)$$

$$P_h = (\Phi_h / \Phi_0) |E_h|^2. \quad (21)$$

### 3. Dynamical thick crystal approximation

The matrix solution obtained in previous section is formally applicable to multilayers with arbitrary thickness. However, the overflow in computer program occurs at small  $\Phi_0$ ,  $\Phi_h < \Phi_c$  when the total thickness of multilayers exceeds  $\sim 10^4$  nm ( $\Phi_c$  is the critical angle of X-ray total external reflection).

This overflow problem is obviously similar to that of calculating the Bragg-case X-ray diffraction from thick crystal plate ( $t \geq 1$  cm). The exponents in some solutions of the dynamical diffraction become so great at the lower surface of the plate that the precision in computations is lost or numerical overflow takes place. These solutions with great exponents are treated as the waves reflected from the lower surface of the plate since their exponents are decreased when  $z$ -coordinate is decreased. Obviously, the amplitudes of these waves are very small and can be put zero in thick crystal. Then, as soon as these solutions are discarded, the boundary conditions at the lower surface can be discarded as well and the effects of lower crystal boundary and the layers below it are neglected. This procedure is known in X-ray optics as the thick crystal approximation.

Let us now turn back to GID in multilayers. At small  $\Phi_0$ ,  $\Phi_h < \Phi_c$  the X-ray wavefield is quickly dampened inside the crystal. That means that several upper layers only contribute to the reflected GID intensity. The reflected waves at lower boundary of some  $k$ -th layer are already so weak (the exponents are so great) that the effect of this boundary and all the layers below it can be neglected. That is the analog of thick crystal approximation. Since the penetration of X-rays in GID strongly depend on  $\Phi_0$ ,  $\Phi_h$ , the number of layers taken into account will vary dynamical from point to point on the diffraction curve. That is why this case can be called *the dynamical thick crystal approximation* [13].

The dynamical thick crystal approximation can be implemented numerically as follows. One can evaluate the maximum matrix element in the right side of (16) after multiplying it by every  $T^k$  starting at  $k = 1$ . As well seen from the example (17), the order of this product at a  $k$ -th interface is  $\simeq \max |(F^k)^{-1}| \simeq \max |\exp(-iu_j^k x z^k)|$ , i.e. just the order of phase exponents is followed. As soon as the product reaches great values (say  $10^{10}$ – $10^{15}$ ), the X-ray waves reflected from the respective interface and

<sup>2</sup> In the case where the measurements of  $P_h$  are carried out depending on  $\Phi_h$  the right side of (21) must be multiplied by  $2 \Phi_h$  (see [15] for details)

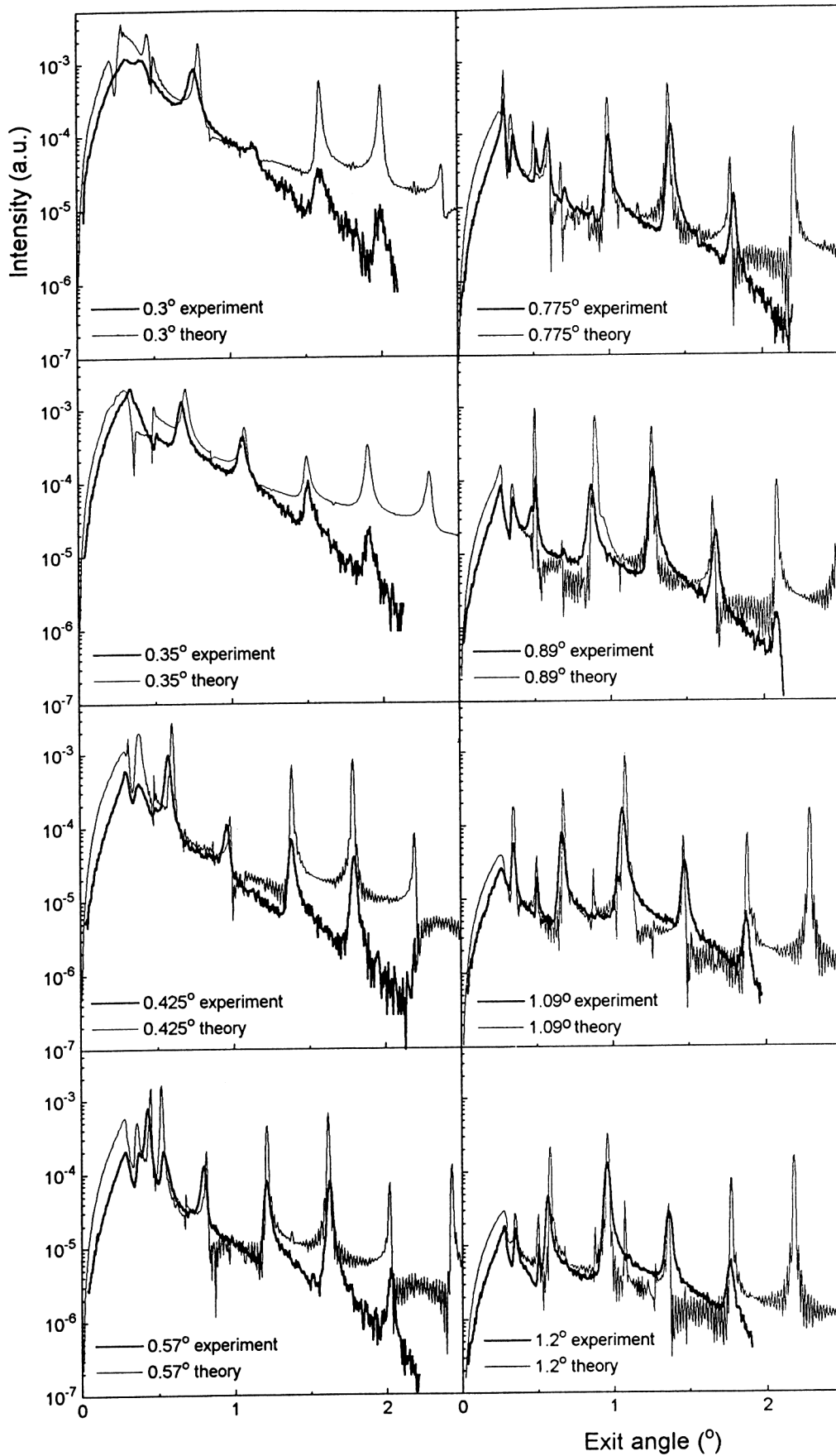


**Fig. 2.** Experimental (thick lines) and computed (thin lines) GID curves taken at several incidence angles from GaAs/AlAs superlattice

the waves reflected from all the deeper interfaces can be neglected. In other words, the layer above this interface can be considered as an infinitely thick substrate and one can take into account in this layer the solutions with  $\text{Im} u_j > 0$  only.

#### 4. Experimental

In the following we compare the formalism given above with the experimental results measured from an AlAs/GaAs superlattice (SL).

Twenty periods of thin GaAs and AlAs layers were grown on GaAs [001] substrate using molecular beam epitaxy. The thickness of the layers in SL was 14.6 nm AlAs and 6.8 nm GaAs as obtained by independent X-ray reflectivity measurements.

The GID experiment was performed at the D4 beam line at HASYLAB using  $\lambda = 0.154$  nm. We measured the GID intensity distributions of the (220) reflection in dependence on  $\Phi_h$  at different fixed  $\Phi_0$ . The angular resolutions, with respect to the incident and diffracted beams, were  $\Delta\Phi_0 = 0.01^\circ$  and  $\Delta\Phi_h = 0.007^\circ$ . The diffracted plane (220) was determined experimentally to be slightly mis-oriented with respect to the surface normal by  $\delta = -0.03^\circ$ . The other details of the experiment are described elsewhere [7].

Some experimental scans recorded at different  $\Phi_0$  are shown by thick solid lines in Fig. 2. All the curves demonstrate well pronounced SL peaks, which document a good periodicity of this structure. Further, some additional effects are observed such as split peaks and shoulders near the SL peaks.

We should note that we failed to explain these additional effects using the kinematical theory of GID proposed in [4].

#### 5. Application of the theory

The calculated curves are shown in Fig. 2 by thin solid lines. These curves were computed assuming a perfect SL structure. Besides, experimental beam spreads were also not taken into account due to the high experimental resolutions  $\Delta\Phi_0$  and  $\Delta\Phi_h$ .

One can see that the computations explain principally all the experimental findings such as peak positions, splitting of the peaks, shoulders etc. The first strong maximum shown at the small angle side of Fig. 2 corresponds to so-called surface (Yoneda) peak. The main peaks at large  $\Phi_h$  are SL peaks caused by the periodicity of SL. These peaks are separated by  $\Delta\Phi_h \approx \lambda/t_{\text{SL}}$ , where  $t_{\text{SL}} = 21.4$  nm is the SL period. The peaks between these regular maxima present the most interest. These peaks observed at both experimental and theoretical curves are due to the multiple reflection of X-ray waves between intrinsic interfaces. These peaks can be explained solely by the dynamical treatment of the diffraction problem. The presence of these peaks on the experimental curves proves the high quality of SL resulted in the dynamical diffraction. Thus, taking into account that the theory assumes a perfect

structure of SL, we can conclude that theory and experiment are in good agreement.

The difference between the experimental and theoretical curves in Fig. 2 is obviously due to various real-structure effects not included in the model used.

For example, the calculated higher-order SL peaks are more intensive than the measured ones. We have checked that this may be caused by interface roughness effect. The account for interface roughness in matrix method and its application to analysis of experimental data will be reported in the next papers [16, 17].

Besides, the slope of the intensity drop in the experimental curves at high  $\Phi_h$  is considerably greater than that in the calculated curves (see especially the curves at  $\Phi_0 = 0.3^\circ, 0.35^\circ$  and  $0.425^\circ$ ). The high slope of the measured curves can be attributed to the limited in-plane divergence of the incident beam at D4 beamline. Furthermore, as known from the reflectivity measurements [18], the surface roughness of the sample can also have a similar effect.

Thus, we have elaborated the dynamical diffraction approach for processing GID measurements taken from various surface multilayer structures including superlattices. The new approach provides explanation to some additional SL peaks and other multi-beam effects which cannot be treated with the kinematical diffraction theory. The account of real-structure effects requires some improvements to our computer program which are possible within the proposed theory. Besides, the further development should include the diffraction in strained and mismatched multilayers. The construction of the respective theory is the subject of our current investigation.

This work was partially supported by the German BMFT under contract number 055IPAA18. The authors are also grateful to D. Martin, EPS Lousanne, Switzerland for the preparation of the sample.

#### References

- Golovin, A.L., Imamov, R.M., Melikyan, O.G.: Sov. Phys. - Appl. Phys. **9**, 95 (1989)
- Golovin, A.L., Imamov, R.M., Melikyan, O.G.: J. Appl. Crystallogr. **22**, 406 (1989)
- Rhan, H., Pietsch, U.: Z. Phys. **B80**, 347 (1990)
- Pietsch, U., Rhan, H., Golovin, A.L., Dmitriev, Yu.: Semicond. Sci. Technol. **6**, 743 (1991)
- Pietsch, U.: Second Int. Conf. on X-ray and Neutr. Scatt., Bad Honnef (Germany) 1991; Zabel, H., Robinson, I.K. (eds.) (Springer proceedings in physics, Vol. 61, p. 53) Berlin: Springer 1992
- Melikyan, O.G., Imamov, R.M., Novikov, D.V.: Solid State Phys. (Russia) **4**, 1572 (1992)
- Pietsch, U., Baumbach, G.T., Martin, D.: HASYLAB'92 Annual Report, Hamburg, Germany 1992
- Rhan, H., Pietsch, U., Rugel, S., Metzger, H., Peisl, J.: J. Appl. Phys. **74**, 146 (1993)
- Pietsch, U., Metzger, H., Rugel, S., Jenichen, B., Robinson, I.K.: J. Appl. Phys. **74**, 2381 (1993)
- Melikyan, O.G.: Kristallografiya (Russia) **36**, 549 (1991)
- Andreeva, M.A., Rosete, C., Khapachev, Yu.P.: Phys. Status Solidi a **88**, 455 (1985)
- Rugel, S., Wallner, G., Metzger, H., Peisl, J.: J. Appl. Crystallogr. **26**, 34 (1993)

13. Stepanov, S.A.: *Kristallografiya (Russia)* **39**, 221 (1994)
14. Aleksandrov, P.A., Afans'ev, A.M., Stepanov, S.A.: *Phys. Chem. Mech. Surf. (U.K.)* **3**, 2222 (1985)
15. Aleksandrov, P.A., Afanas'ev, A.M., Golovin, A.L., Imamov, R.M., Novikov, D.V., Stepanov, S.A.: *J. Appl. Crystallogr.* **18**, 27 (1985)
16. Stepanov, S.A., Köhler, R.: *First Europ. Conf. on Synchrotron Radiation in Materials Science, Chester (U.K.)*, P7.10 (1994); *J. Appl. Phys.* (submitted for publication)
17. Jenichen, B., Rhan, H., Stepanov, S.A., Ohler, M., Köhler, R.: *The 2nd Europ. Symposium on X-Ray Topography & High Resolution Diffr., Berlin, Germany, 1994*
18. Ming, Z.H., Krol, A., Soo, Y.L., Kao, Y.H., Park, J.S., Wang, K.L.: *Phys. Rev.* **B47**, 16373 (1993)